

PID TUNING BY CENTRAL COMPOSITE ROTATIONAL DESIGN METHODOLOGY: A CASE STUDY OF ABSORPTION COLUMN FOR BIOGAS PURIFICATION

CLAUDIA LUIZA MANFREDI GASPAROVIC¹, EDUARDO EYNG^{1,*}
LAERCIO MANTOVANI FRARE¹, RAFAEL ARIOLI¹ AND FABIO ORSSATTO²

¹Postgraduate Program in Environmental Technologies

²Academic Department of Biological and Environmental Sciences
Federal University of Technology – Parana

No. 4232, Brazil Avenue, Medianeira, Parana 85884-000, Brazil

*Corresponding author: eduardoeyng@utfpr.edu.br

Received May 2017; revised September 2017

ABSTRACT. *Control systems are a tool of major potential in the environmental field, and among them, the most widely used type is the Proportional Integral Derivative (PID) controller. However, its operation depends on parameters (K_c , τ_I , and τ_D), which usually may be adjusted by trial and error, in an expensive process. The objective of this study was to use the experimental design methodology, through a Central Composite Rotational Design (CCRD), to tune the parameters of a PID controller, while applying the control system to an absorption column for biogas purification, simulated through a mathematical model. The regulatory problem was addressed through a feedback controller, whose performance was evaluated by the ITAE criterion (Integral of Time weighted by the Absolute Error). The experimental design matrix consisted of 23 factorial runs, six runs in the axial points and three repetitions at the central point. The response variable was the ITAE criterion, and the factors were the controller parameters. The quadratic model fitted for ITAE response was proven valid and predictive for the study range, through an analysis of variance. The optimal values of controller parameters, found through the CCRD, made the controller able to keep the system stable, even with the insertion of various disturbances.*

Keywords: Biogas purification, Biomethane, Experimental design

1. Introduction. The use of control systems has numerous applications in the environmental field and may prove to be very useful in situations such as pollutant minimization and increase of process efficiency. Among the controller types, the most widely used is the PID controller (Proportional Integral Derivative), because of its proven effectiveness as well as the relative simplicity required for its operation [1].

The design of these controllers requires the determination of three parameters: proportional gain (K_c), integral gain (τ_I) and derivative gain (τ_D), which are adjusted in each case in a process called tuning [2]. Finding satisfactory values for these parameters is not an easy task without a systematic procedure [3]. Several studies have been published in recent decades which present methodologies for the tuning of PID parameters, such as methods based on mathematical models, with highlights to the works of Ziegler-Nichols [4], Cohen and Coon [5] and López et al. [6], as appointed by [7].

Such methods, however, only provide an initial estimate of the parameters, requiring a further fine-tuning commonly done by trial and error, thus spending time and resources [2,8-10]. Several strategies have been proposed in recent years to replace the traditional models, such as automatic tuning, artificial neural networks, FOPTD (First Order Plus

Time Delay), and EVRFT (Enhanced Virtual Reference Feedback Tuning) [1,11], and as such, the search for alternative tuning techniques is a promising research field.

It is desirable for industrial processes control systems to be able to meet servo and regulatory problems; however, each of these applications will have an optimal set of values for the parameters, requiring a global optimum solution [12,13].

Single-input single-output PID controllers have been used for Multiple-Input Multiple-Output (MIMO) plants for many years. For MIMO plants that are already reasonably well-decoupled, multi-loop SISO PID design can work well. An alternative to multi-loop SISO PID control is to design one MIMO PID controller, which uses matrix coefficients, all at once. The challenge is in tuning MIMO PID controllers, which require the specification of three matrices, each with a number of entries equal to the number of plant inputs times the number of plant outputs [14].

In this sense, the controller parameters tuning becomes an even more complex task, which reinforces the applicability of experimental planning methodologies as tools for PID controller tuning process.

Empirical modeling can be used to analyze systems or processes when multiple variables (factors) may exert significant effects on their responses. For that, it is increasingly common to make use of experimental design, a tool that allows to obtain optimal results while requiring less runs.

The Central Composite Rotational Design (CCRD) is one of the most useful experimental planning methodologies when there are two or three factors. In this way, CCRD may be used to evaluate the optimal values for a set of controller parameters (K_c , τ_D and τ_I), which provide the best result to a performance criterion, such as the integral of time-weighted absolute error – ITAE. This method can also be applied to a simultaneous optimization process, i.e., when searching for optimal values of controller parameters for both regulatory and servo problem. Therefore, another process response would be added: ITAE for regulatory problem and ITAE for servo one.

In order to test the experimental design methodology CCRD as a tool to optimize the PID controller parameter tuning process, a study case in the environmental field is presented, in which a tray absorption column aimed at removing CO₂ from biogas was simulated through a mathematical model. A PID controller was implemented and its parameter tuning was made by CCRD.

A diversification in the global energy matrix is needed and biogas is one of the most promising alternative sources. It is a gas mixture consisting primarily of Methane (CH₄), Carbon Dioxide (CO₂) and Hydrogen Sulfide (H₂S), produced from the anaerobic digestion of organic matter from waste treatment processes (urban, agricultural, etc.) – another environmental benefit. It may be used in various ways depending on its composition and purity [15].

Several studies have been done regarding H₂S removal from biogas, due to its corrosive characteristics. However, removal of CO₂ also presents great advantages, since once the other gases are removed, it is possible to obtain biomethane, a product with very similar characteristics to natural gas and that can replace it. To be considered biomethane, according to recommendations of the National Petroleum Agency of Brazil (ANP Resolution N°8 01.30.2015) biogas should have a carbon dioxide concentration of 3% maximum.

One of the technologies that can be used to remove CO₂ from biogas is a tray absorption column. The basic operation of this equipment consists in the contact between a liquid stream, which by concentration gradient will absorb a particular pollutant present in a counter-current flow of gas stream. In this study, a pressurized column was chosen, to increase the efficiency of CO₂ removal, and the liquid stream was water.

The required liquid flow depends on several factors, such as solute concentration in the two phases, solute equilibrium between the two phases, and inlet CO_2 concentration. The non-compatibility of these two parameters (water flow and CO_2 concentration in biogas) impairs the system's operation, leading to waste of liquid stream in one case, or to reduction in treatment efficiency in the other. Both situations provide loss of environmental quality, hence explaining the importance of the use of a PID controller in this system.

This paper is organized according to the following aspects: (1) An experimental design methodology, Central Composite Rotational Design, was used to provide an efficient PID controller tuning with fewer runs; (2) The applicability of this tuning methodology was tested in a study case in the environmental field; (3) A tray absorption column is supposed to make feasible the contact between biogas and water (solvent) flow rates in order to reduce the CO_2 concentration in the outlet gas stream; (4) A PID controller was implemented in the simulated absorption column to manipulate the inlet water flow rate to ensure efficient biogas purification and also water saving; (5) After a first estimation of K_c , τ_D and τ_I values, the independent variables ranges were defined, as well as the experimental design matrix; (6) The integral of time-weighted absolute error – ITAE was used to evaluate the controller performance; (7) A quadratic model (function of the factors K_c , τ_D and τ_I) for ITAE was fitted from the tests results; (8) The PID tuning was made based on the quadratic model for ITAE, on an optimization process.

2. Materials and Methods.

2.1. Studied system characterization. The studied system was composed of a tray absorption column, through which compressed biogas flows upward, and water downward, aiming to remove carbon dioxide present in biogas. Figure 1 illustrates the equipment and utilities arrangements for the purification.

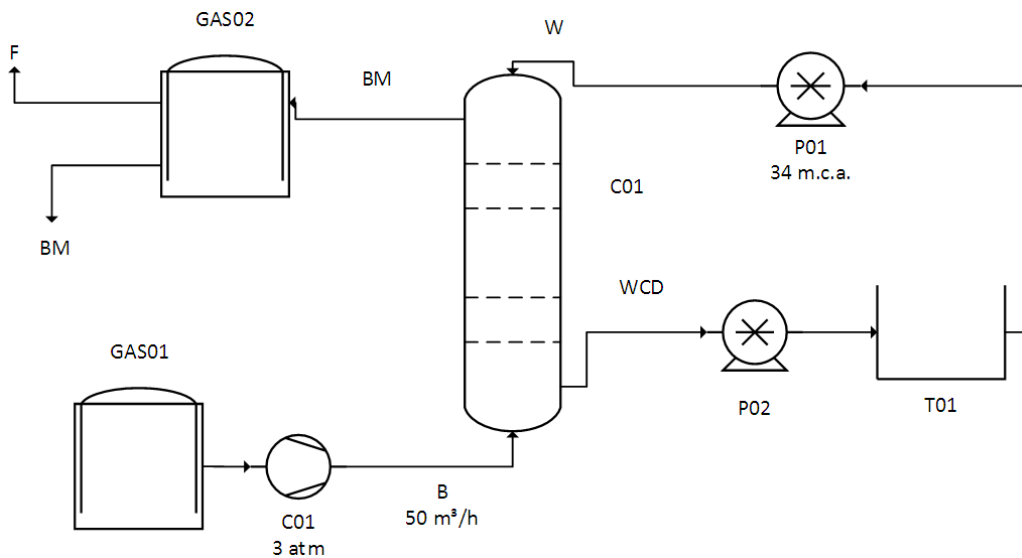


FIGURE 1. Equipment and utilities chart

In Figure 1, the following abbreviations are used: B, biogas; BM, biomethane; C01, absorption column; T01, reservoir tank of water; P01, water inflow pump; P02, water outflow tank; GAS01, reservoir tank of biogas; C01, compressor; GAS02, reservoir tank of biomethane; W, water; WCD, water with carbon dioxide dissolved; F, flare.

In the system represented in Figure 1, water inflow is manipulated to control the dissolved carbon dioxide in the biogas outflow according to the set point.

While the system is undisturbed and without the controller's actions (open loop), the water flow, corresponding to $2783 \text{ cm}^3 \cdot \text{s}^{-1}$ (about $10 \text{ m}^3 \cdot \text{h}^{-1}$) is moved from a T01 tank to the highest elevation by pump P01, overcoming a positive shift of about 34 w.c.m. In closed loop the water flow is controlled by the PID controller. Biogas originated from biogas reservoir GAS01 is sent to the column at a flow rate of $50 \text{ m}^3 \cdot \text{h}^{-1}$ by a compressor C01, which compresses it at 3 atm.

The effluent water flow of about $27.5 \text{ m}^3 \cdot \text{h}^{-1}$ ($17.5 \text{ m}^3 \cdot \text{h}^{-1}$ of it corresponding to CO_2) is returned to the T01 tank to be decompressed and release CO_2 . Effluent biomethane (flow of $33.2175 \text{ m}^3 \cdot \text{h}^{-1}$ in a scenario without disturbances, corresponding to methane flow plus 3% CO_2) is sent to biogas reservoir GAS02 and subsequently forwarded for sale. The biogas reservoir GAS02 has a flare burner for emergencies and excesses burning.

2.2. Absorption column modeling and simulation. The dynamic model developed by Maia [16] was used to perform the modeling and simulation of the absorption column. The model refers to a column with N plates, where there is physical absorption of a gas component. Plates are numbered in descending order, in that gas feeding takes place at the N -th plate, and liquid in the first plate.

The model was obtained from the overall mass balances for each stage n , mass balances for the component which is absorbed in each stage n , equilibrium relationship and Francis equation.

CO_2 solubility in water for the described conditions was calculated by the equilibrium equation $Y = 545 X$, where X is the CO_2 mole fraction in the liquid phase, and Y is the CO_2 mole fraction in the gas phase. The equilibrium relationship was obtained through Henry's Law, Henry's constant values for CO_2 and the system pressure.

For the column mathematical model, the following simplifications were used [17]: 1) Only one component is transferred from one phase to another; 2) Absorption is considered isothermal; 3) Each stage is considered as ideal; 4) Solute transferring between phases does not change gas or liquid flows; 5) Pressure is constant along the column; 6) It is assumed no amount of gas is trapped between stages.

For the study, the composition considered for the biogas is shown in Table 1.

TABLE 1. Biogas composition considered for the study

Component	Concentration (% in volume)
Methane (CH_4)	64.5
Carbon dioxide (CO_2)	35
Hydrogen sulfide (H_2S)	0.5

To achieve molar balance, biogas was considered as a binary mixture of carbon dioxide and other gases classified as "non-carbon-dioxide", i.e., methane majority, and hydrogen sulfide as a small fraction. In the simulation absolute values for both flows and the fractions moles of the component were used. Table 2 shows the values used for absorption column parameters.

The column parameters were determined as follows: the operation temperature corresponds to the average temperature of the region in which the study was carried out, which is an area of great potential for biogas production; the gas flow rate was adopted from empirical values of the amount of biogas produced in a rural property in said region; the operation pressure was selected according to literature data, such as [18-20]; the water flow rate was estimated according to Magalhães et al. [20] and the number of ideal stages (N) was calculated through equilibrium equation and mass balances; and the sizing and project were carried out according to Spellman and Whiting [21].

TABLE 2. Absorption column parameters

Parameter	Value
Temperature	25°C
Pressure	3 atm
Plate area	210 cm ²
Spillway height	8 cm
Number of ideal stages (N)	5
Gas flow (G)	0.1987 mols.s ⁻¹
Initial liquid flow (L0)	154.5914 mols.s ⁻¹
CO ₂ concentration in the affluent liquid (X0)	0
CO ₂ concentration in the affluent gas (Y6)	0.5394 mols.s ⁻¹

Through the Francis equation, an equation for liquid retention in the plate was reached, and by isolating the liquid flow leaving each plate, Equation (1) is obtained:

$$L_n = \rho_n L_W \left[\frac{1}{c} \left(\frac{M_n}{P_a \rho_n} - s_h \right) \right]^{\frac{3}{2}} \quad (1)$$

where:

ρ_n = Average specific molar mass of the mixture (moles/cm³)

P_a = Plate area (cm²)

c = Constant (cm^{-1/3}s^{2/3})

s_h = Spillway height (cm)

L_W = Spillway length (cm)

L_n = Liquid flow leaving each plate (cm³s⁻¹)

Controller programming and simulation applied to the column were developed in MATLAB software R2013b version.

2.3. Absorption column control. Control of the absorption column was carried out using a PID feedback controller, and the column regulatory problem was addressed. The manipulated variable is the affluent water flow to the column, and the controlled variable corresponds to the component (CO₂) concentration in the gas stream effluent to the column. The value of the controlled variable should remain close to the set point value (desired value for CO₂ mole fraction in biomethane). The set point value, as previously defined, was 3%, which is equivalent to an absolute concentration of 0.0309 (mols of CO₂).(mols of liquid)⁻¹.

The PID controller applied to the regulatory problem for the absorption column had its modeling performed from the control law, which led to Equation (2):

$$L_0(kSt) = L_0(kSt - St) + K_c e(kSt) + \frac{St}{\tau_I} \sum_{i=0}^k e(iSt) + \tau_D \left(\frac{e(iSt) - e(iSt - 1)}{St} \right) \quad (2)$$

where L_0 is the solvent flow at column entrance; k is the sampling instant; St is the sampling time; K_c is the controller gain; τ_I is the integral time constant; τ_D is the derivative time constant; e is the error.

The step of tuning the controller parameters refers to finding optimal values for constants K_c , τ_D and τ_I . The numerical values for proportionality constants K_c , τ_D and τ_I were defined using the experimental design methodology through a Central Composite Rotational Design whose study range was defined from an initial estimate.

The initial estimate was made using the method proposed by López et al. [6], based on ITAE performance criterion, which uses Equations (3), (4) and (5):

$$K_c = \frac{a_1}{K_p} \left(\frac{t_d}{\tau_p} \right)^{b_1} \quad (3)$$

$$\tau_I = \frac{\tau_p}{a_2} \left(\frac{t_d}{\tau_p} \right)^{b_2} \quad (4)$$

$$\tau_D = a_3 \tau_p \left(\frac{t_d}{\tau_p} \right)^{b_3} \quad (5)$$

where K_p is the process gain, t_d the dead time of the process, τ_p the time constant and the values for coefficients a_1 , a_2 , a_3 , b_1 , b_2 and b_3 are shown in Table 3 [6].

TABLE 3. Equation coefficients values

Coefficient	Value
a_1	1.357
a_2	0.842
a_3	0.381
b_1	-0.947
b_2	-0.738
b_3	0.995

Source: López et al. [6]

Values for K_p , t_d and τ_p were obtained through the analysis of the response graph (controlled variable) of a simulation performed in open loop in which a 20% negative perturbation has been inserted in the manipulated variable, at instant 5 s. Thus, water inflow value was reduced by 20% from that moment on. In Figure 2 it can be seen from the chart how the parameters were obtained.

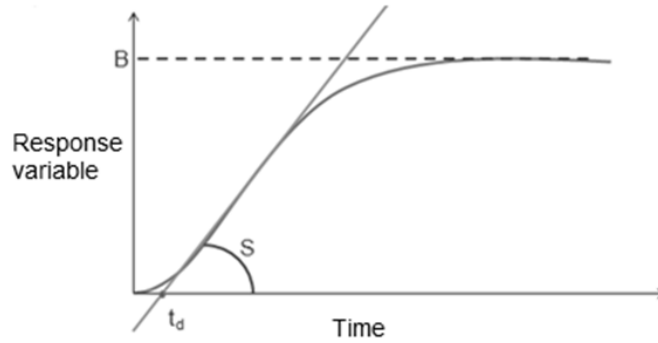


FIGURE 2. Chart for parameters estimation

In Figure 2, the following abbreviations were used: B, response value after system stabilization; t_d , point where the tangent line to the inflection point of the curve intersects time axis (located on the ordinate corresponding to the set point); S, angular coefficient of the tangent line.

The K_p value is obtained from the ratio between A and B, where A corresponds to the magnitude of the disturbance applied to the manipulated variable (in the same unit as the variable), and B is the response value after system stabilization. τ_p value is then obtained from the ratio between B and S.

3. Evaluation of CCRD as a PID Tuning Methodology.

3.1. Experimental design. The performed CCRD was a factorial design 2^3 , with eight factorial runs, six axial point runs, and three repetitions at the central point. The independent variables were the controller parameters K_c , τ_D and τ_I .

The response variable was the ITAE performance criterion, which is the absolute error integral weighted for time, shown by Equation (6).

$$ITAE = \int |e|.tdt \quad (6)$$

where e is the error, i.e., the difference between the controlled variable and set point; t is time. The experimental design runs were performed using simulations in a program developed on the software MATLAB. All runs were performed with the same conditions, which are presented in Table 4.

TABLE 4. CCRD simulation conditions

CO ₂ initial normal mole fraction	0.35
Disturbance CO ₂ normal molar fraction	0.4
Disturbance instant	100 s
Maximum time simulation	3000 s

The system is initially at set point, wherein the biogas entering the column has a CO₂ concentration of 35%, and biomethane leaving the column has the desired concentration of 3% CO₂. At time equal to 100 s, it is inserted a disturbance in the affluent biogas CO₂ concentration in that it rises from 35% to 40%. It produces, as effect, an effluent gas whose CO₂ concentration higher than desired (set point), until the controller gets into action.

The results obtained with the CCRD were analyzed with the Statistica v.7 software in order to obtain a predictive model for the ITAE value as a function of the parameters K_c , τ_D and τ_I .

The obtained model makes it possible to find an optimal set of controller parameters to minimize ITAE value, i.e., improving controller performance.

3.2. Initial estimation of controller parameters. The implementation of the column modeling program using the MATLAB environment enabled to simulate its operation for given disturbances. The graph used to obtain the parameters for the initial estimation of controller parameters, generated by inserting the disturbance in the manipulated variable, can be found in Figure 3.

In Figure 3, the line corresponds to the molar concentration of carbon dioxide dissolved in the biomethane that leaves the column.

The values of A, B and S obtained from the results shown in the graph, the values for t_d , K_p and τ_p , used for the estimation, and the initial estimates results for the K_c , τ_I and τ_D controller parameters are shown in Table 5.

A system simulation was performed with the values of the initial estimate for the controller and it was obtained of an ITAE value equal to 0.44346, with CO₂ concentration value of exiting gas approaching the set point around 3000 s. Overshoot reached close to 0.037 mols.s⁻¹ in absolute fraction, which corresponds to 0.356 normal fraction. The initial parameters simulation is shown in Figure 4.

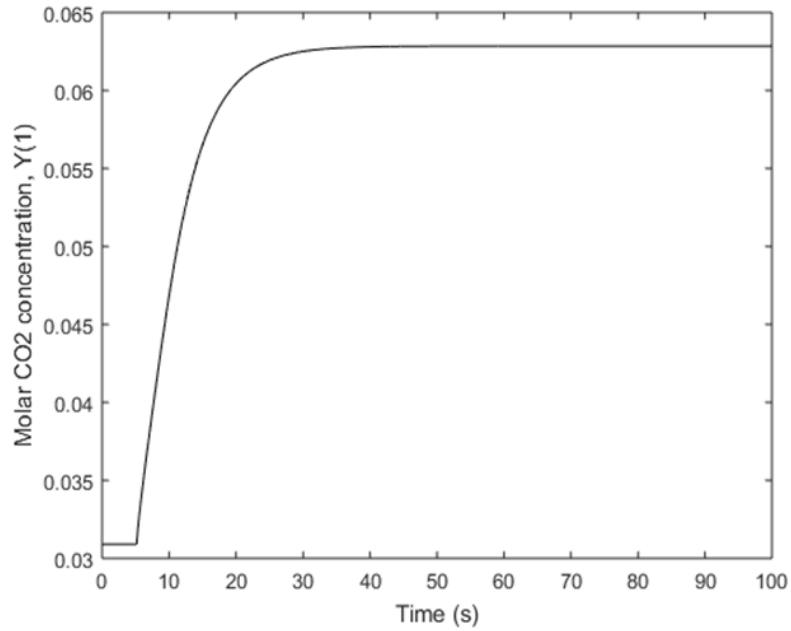


FIGURE 3. Graph for determination of constants for the initial estimate

TABLE 5. Initially estimated controller parameters

Values obtained from the graph (mols/s)		Estimate parameters		Initial estimate controller parameters	
A	30.92	K_p	0.062	K_c	948.89
B	0.0628	t_d	0.4	τ_I	479.88
S	0.0029	τ_p	21.414	τ_D	0.155

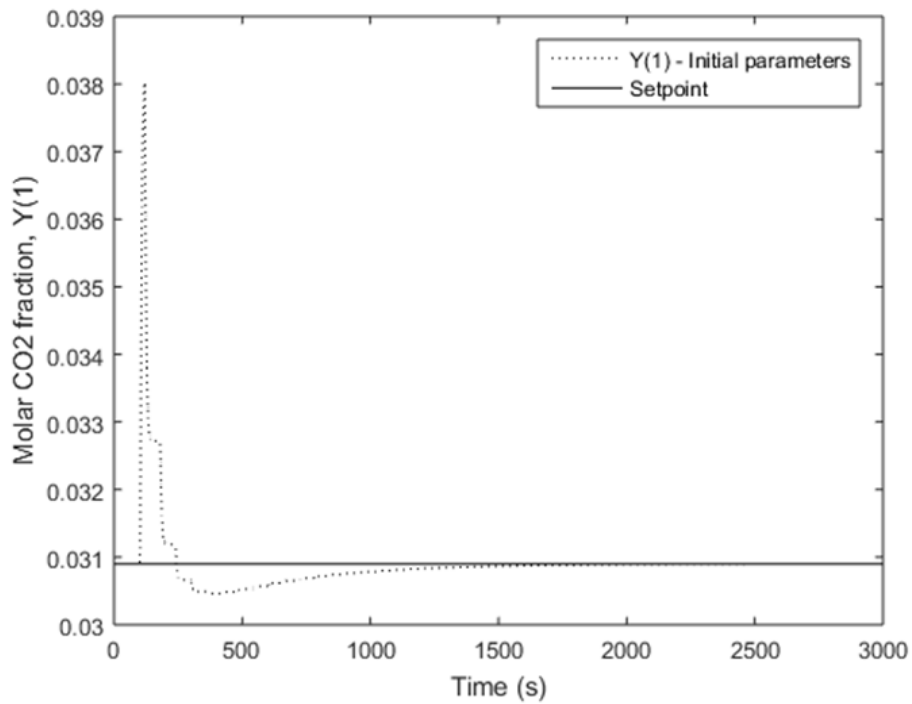


FIGURE 4. Column control simulation with the estimated initial values of controller parameters

In Figure 4, the dotted line corresponds to the molar concentration of carbon dioxide dissolved in the biomethane that leaves the column, and the continuous line to the set point.

3.3. Experimental design matrix and effects of studied variables. CCRD study ranges were set from the initial estimates and preliminary tests. The criterion used was to take approximately twice the amount of the initial estimate for the upper limit, and half for the lower range limit. Since the lower value for τ_D would be close to zero, the study range was extended to zero for this parameter.

By definition of the used method (CCRD) and number of variables, the encoded value to the upper limit of the range corresponds to +1.68, and the lower limit corresponds to -1.68. To obtain the decoded intermediate range values for the variables, linear interpolations were performed, according to Equations (7), (8) and (9):

$$K_{c_{real}} = 424.1K_{c_{cod}} + 1187.5 \quad (7)$$

$$\tau_{I_{real}} = 214.3\tau_{I_{cod}} + 600 \quad (8)$$

$$\tau_{D_{real}} = 0.089\tau_{D_{cod}} + 0.15 \quad (9)$$

Study ranges for K_c , τ_I and τ_D variables of CCRD are presented in Table 6.

TABLE 6. Real and encoded values of variables used in the CCRD methodology

	-1.68	-1	0	1	1.68
K_c	475	763.4	1187.5	1611.6	1900
τ_I	240	385.7	600	814.3	960
τ_D	0	0.061	0.150	0.239	0.300

The experimental design matrix and the results obtained from simulations with the conditions set out in CCRD are shown in Table 7.

TABLE 7. Experimental design matrix and simulation results using the CCRD

Run	K_c	τ_I	τ_D	ITAE
1	-1	-1	-1	0.6023
2	+1	-1	-1	0.1979
3	-1	+1	-1	0.6547
4	+1	+1	-1	0.1995
5	-1	-1	+1	0.6017
6	+1	-1	+1	0.1978
7	-1	+1	+1	0.6541
8	+1	+1	+1	0.1995
9	0	0	0	0.2879
10	0	0	0	0.2879
11	0	0	0	0.2879
12	+1.68	0	0	0.2641
13	-1.68	0	0	1.1632
14	0	+1.68	0	0.2879
15	0	-1.68	0	0.2679
16	0	0	+1.68	0.2874
17	0	0	-1.68	0.2883

Test responses ranged from 0.1979 to 1.1632, and the lowest found value represents about 55% improvement in ITAE in comparison to the simulation using the initial estimated values. There was no noticeable variation among the central points, indicating good process repeatability, which was to be expected given it is a simulation.

It is noticed that in general a setting that features higher ITAE value tends to need more time to reach set point after a disturbance. For example, with the configuration of run 13, 1900 seconds are necessary, whereas in run 9 it takes about 1100 seconds.

It is also important to note the relation between the ITAE value and the time during which the controller's response is above the set point. With the configuration of run 13, the controller's response was held for about 300 seconds above the set point, while in trial 7 it held about 200 seconds, and in trial 9 for about 100 seconds.

Thus, analyzing CCRD results shown in Table 7, it was possible to calculate the effects of the three studied variables, which are presented in Table 8.

TABLE 8. Effects of studied variables on CCRD for the ITAE performance criterion response

Factors	Effect ^a	Standard error	$t(7)$	p -value
Mean ^{b,c}	0.289338	0.022779	12.7021	$4.33 \times 10^{-6*}$
$K_c(L)$	-0.473263	0.021407	-22.1081	$9.78 \times 10^{-8*}$
$K_c(Q)$	0.292010	0.023583	12.3821	$5.15 \times 10^{-6*}$
$\tau_D(L)$	0.020750	0.021407	0.9693	0.3647
$\tau_D(Q)$	-0.016808	0.023583	-0.7127	0.4991
$\tau_I(L)$	-0.000393	0.021407	-0.0183	0.9859
$\tau_I(Q)$	-0.009711	0.023583	-0.4118	0.6928
K_c by τ_I	-0.025401	0.027957	-0.9086	0.3938
K_c by τ_D	0.000258	0.027957	0.0092	0.9929
τ_I by τ_D	0.000005	0.027957	0.0002	0.9998

^aEffects presented in seconds; ^bL = linear terms; ^cQ = quadratic terms; * $p \leq 0.05$.

3.4. Quadratic model for ITAE. The results from the experimental runs also allow to obtain a quadratic model of ITAE as a function of the statistically significant variables, as well as the optimal values for the PID parameters. Figure 5 shows the Pareto chart for the experimental design matrix, which allows a more clear observation of which model parameters are significant.

In Figure 5, the bars indicate which parameters had its p -value inferior to the significance level, shown in the dashed line.

As it is seen in the chart, among the studied variables, only the linear and quadratic terms of K_c parameter (controller gain) were statistically significant, presenting a p -value lower than the significance level (5%). Thus, the other two parameters can be fixed at any point within the study range. For τ_D , that means it can be placed at the encoded value -1.68, which corresponds to the real zero, and as it is, it does not influence significantly on the system control.

The analysis of the experimental design results allowed to determine the regression coefficients shown in Table 9, in order to obtain a quadratic model for the response (ITAE performance criterion), as a function of the significant parameters related to the studied variables.

It is observed that the p -value for the significant terms was much lower than 0.05, confirming its significance. It is also important to notice the low standard error values for the terms, of less than 1%. The model shown in Equation (10) was obtained from

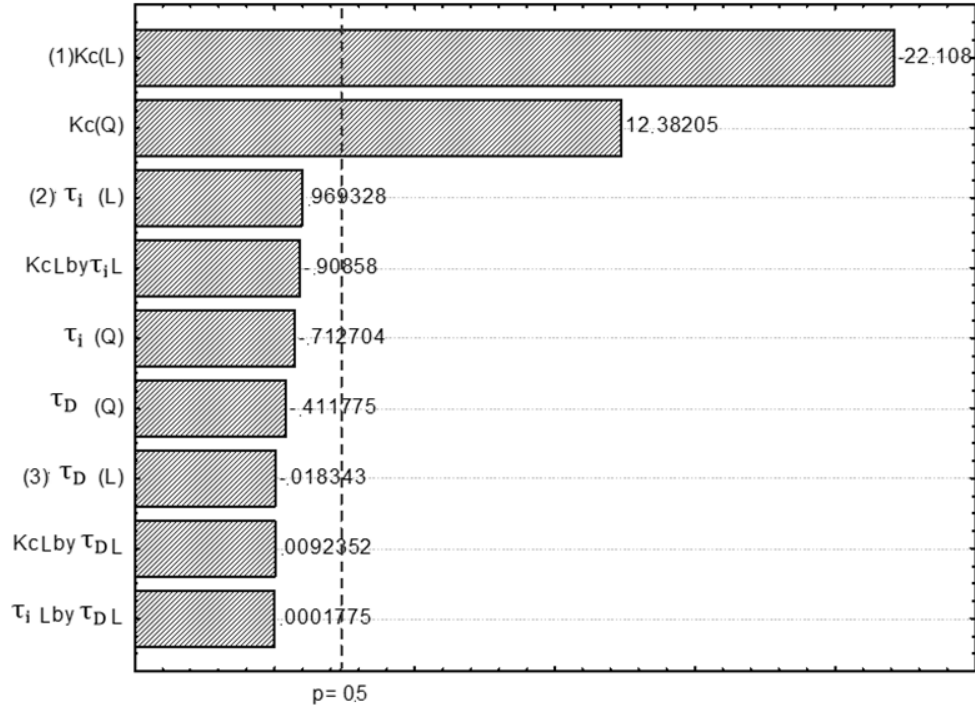


FIGURE 5. Pareto chart for the experimental design matrix

TABLE 9. Regression coefficients for the ITAE performance criterion response

	Regression coefficients	Standard error	$t(14)$	p -value
Mean	0.276275	0.010623	26.0083	2.98×10^{-13}
$K_c(L)$	-0.236632	0.008732	-27.0989	1.69×10^{-13}
$K_c(Q)$	0.149020	0.008953	16.6448	1.28×10^{-13}

* $p \leq 0.05$; L – linear terms; Q – quadratic terms.

TABLE 10. ANOVA for the quadratic model of the ITAE criterion as function of the significant terms

Variation source	SQ ^a	GL ^b	QM ^c	$F_{\text{calculated}}$	$F_{\text{tabulated}}$	p -value
Regression	1.052284	2	0.526142144	505.700	3.74	8.84×10^{-14}
Residues	0.014566	14	0.001040424			
Total	1.066850	16				

% explained variation (R^2) = 98.63%; ^a = square sums; ^b = degrees of freedom; ^c = mean squares.

the statistically significant parameters, and describes the ITAE value as a function of the encoded K_c value.

$$ITAE = 0.276275 + 0.14902K_c^2 - 0.236632K_c \tag{10}$$

The non-significant parameters were added to the residue for the analysis of variance (ANOVA), as shown in Table 10, in order to determine the statistical significance of the model.

It can be seen that the F test value (505.7) for the regression was highly significant (p -value 8.84×10^{-14}), about 135 times higher than the critical value (3.74) which is

adequate, taking account of that to validate the model, the calculated F should be at least 4 to 5 times higher than the critical value [22]. Variance percentage explained by the model was also adequate ($R^2 = 98.63\%$), almost reaching 99%. Thus, the model is predictive for the study range.

3.5. Optimal regions and values for the PID parameters. The model was used to generate response surface and contour lines charts. Surfaces were generated as a result of K_c and τ_I or τ_D , setting the remaining variable at the central point. Figure 6 shows the ITAE response surface as a function of K_c and τ_I , with τ_D set at central point, and below is the ITAE response surface as a function of τ_D , with τ_I fixed at central point.

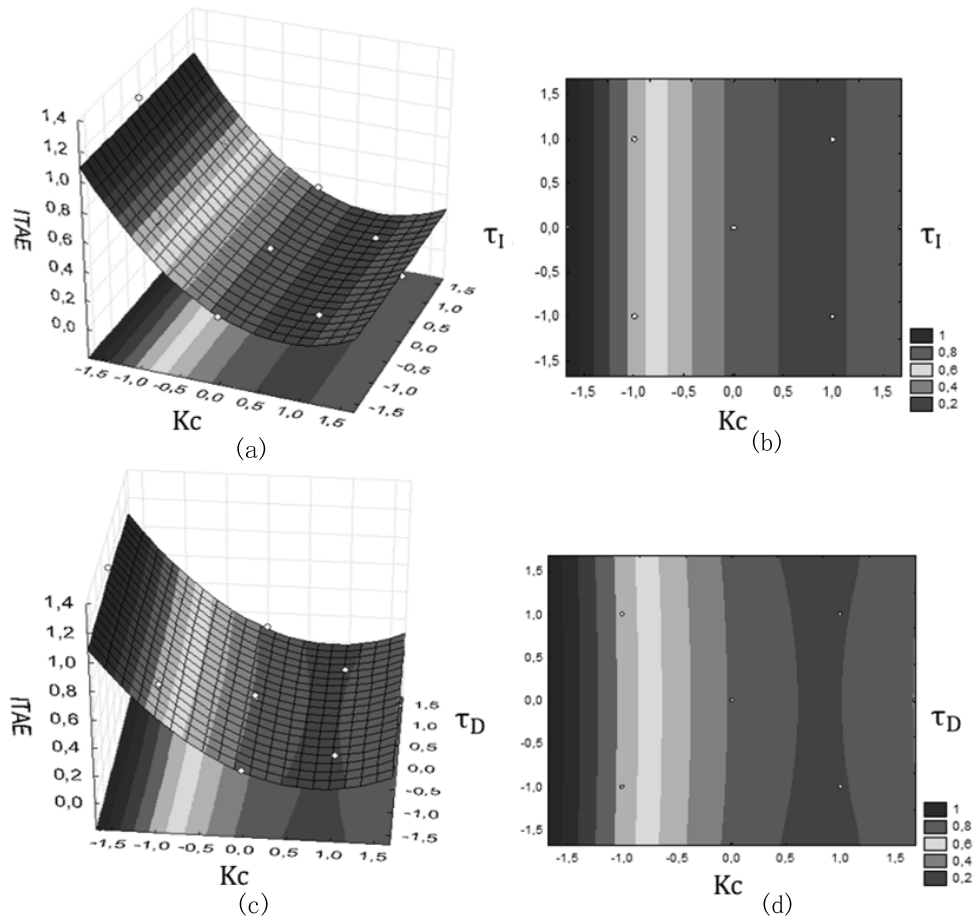


FIGURE 6. ITAE response surfaces and contour lines

In it Figure 6(a) corresponds to the response surface of ITAE as a function of K_c and τ_I , with τ_D fixed in the central point; Figure 6(b) to the contour plot of ITAE as a function of K_c and τ_I , with τ_D fixed in the central point; Figure 6(c) to the response surface of ITAE as a function of K_c and τ_D , with τ_I fixed in the central point; and Figure 6(d) to the contour plot of ITAE as a function of K_c and τ_D , with τ_I fixed in the central point.

The response surfaces and contour lines presented indicate that the optimal range for K_c , the only significant variable, is between approximately 0.5 and 1.1 for coded values, which represent 1400 to 1654 in real values.

The optimal value for K_c was found in order to optimize the process and to validate the model in experimental conditions. To this end the model was derived and the derivative was equal to zero, for it represents a point of minimum on the curve. As the τ_D and τ_I variables were proven not to be significant, they are not included in the model and were

TABLE 11. Real and coded values of optimal conditions

Value	K_c	τ_I	τ_D
Coded	0.79396	0	0
Real	1524	600	0.15

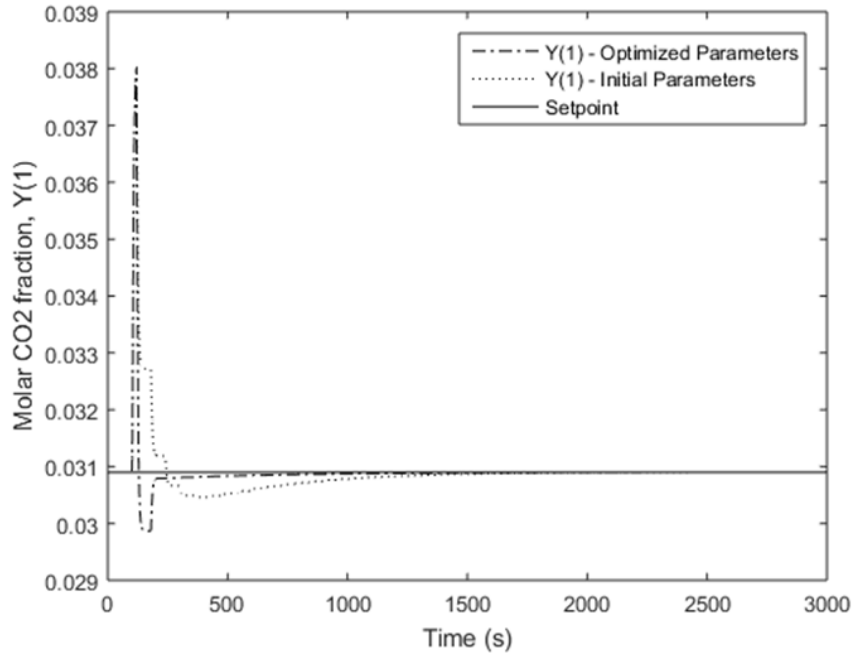


FIGURE 7. Simulation to validate optimal conditions

fixed in the central points of the study range. Real and coded values for the variables optimal conditions are presented in Table 11.

Validation of the optimal values for the PID parameters. To validate the controller's optimal conditions, a simulation with the same conditions used in the CCRD was carried out. The response chart of this simulation is shown in Figure 7 along with the simulation response for the initial parameters, under the same conditions, for comparison.

In Figure 7, the dotted line corresponds to the molar concentration of carbon dioxide dissolved in the biomethane that leaves the column, when the initial parameters are used; the dashed-dotted line corresponds to the molar concentration of carbon dioxide dissolved in the biomethane that leaves the column, when the optimized parameters are used; and the continuous line corresponds to the set point.

The controller's time response chart indicates very good performance, highlighting the low time to reach set point and the very low time that the controlled variable remains above the set point (30 seconds). By analyzing the chart, it is expected that the ITAE value would also be low, given the small area covered by the curve.

The simulation enabled to find the ITAE value for the configuration, which was compared to the value predicted by the model for the optimal condition. Results as well as the model prediction error are shown in Table 12.

The value predicted by the model was very close to the real value obtained from the simulation. The difference was just over a tenth, representing approximately 8.65% of the actual value. The model prediction error was less than 10%, confirming proper model adjustment to the experimental data. Thus, as indicated by the ANOVA, the model is indeed valid and predictive for the study range.

TABLE 12. Model validation in optimal conditions

ITAE value using the initial estimated values for the parameters	ITAE value predicted by the model for the simulation in the optimal conditions	ITAE value obtained from the simulation in the optimal conditions	Model prediction error (%)
0.44346	0.182337	0.199602	8.65%

It was also noted that the ITAE value obtained with the simulation in optimal conditions represented a 50% reduction in the value obtained using the values initially estimated for the parameters, which indicates a significant improvement in the controller performance.

3.6. Performance assessment of the tuned PID controller. After proving the quadratic model validity, it is necessary to prove the proposed control system effectiveness with optimized parameters. Therefore, it would be appropriate to verify how it performs with disturbance values different from those used in the experimental design.

Thus, other simulations were carried out, whose ITAE conditions and resulting value are presented in Table 13. In order for the tests to have a good coverage, it was used positive (runs 1 and 2) and negative (run 3) disturbances, and also, a simulation with a positive disturbance followed by a negative disturbance after the stabilization of the first one (run 4).

TABLE 13. Simulations for control system checking

Run	Time of disturbance insertion	Maximum Simulation Time	Normal CO ₂ mole fraction in biogas prior to disturbance	Normal CO ₂ mole fraction in biogas, Y(6), after disturbance	ITAE for the initial parameters	ITAE for the optimized parameters
1	100	3000 s	0.35	0.45	0.9046	0.4925089
2	100	3000 s	0.35	0.5	1.1779	0.9892596
3	100	3000 s	0.35	0.25	1.4110	0.5885905
4	100 1500	3000 s	0.35	0.4 0.3	2.4740	1.541141

ITAE values of runs with the optimized parameters remained low, presenting the same order of magnitude as those obtained with the CCRD, even with more significant or negative disruptions. The only run in which ITAE value was superior to the maximum obtained with the CCRD was the fourth run, in which two disturbances were inserted. In comparison, runs with the initial parameters obtained higher ITAE values in all simulations. The controller performance in each case becomes more visible observing the (absolute) molar fraction charts of CO₂ in biomethane over time.

Figure 8 corresponds to the controller response graph for run 1.

It is noticed that for run 1, with a disturbance about 15% higher than the one implemented in the CCRD, the controller with optimized parameters also acted efficiently, as it required a low time to reach the set point, presenting few fluctuations. When compared to the initially estimated values, one can see a 45% reduction in the ITAE value. The superior performance for the controller with optimized parameters can also be verified in Figure 8, since it clearly presents fewer errors and takes less time to return to set point. With the initial parameters the controller takes about 1500 s, whereas with optimized parameters it requires only about 250 s.

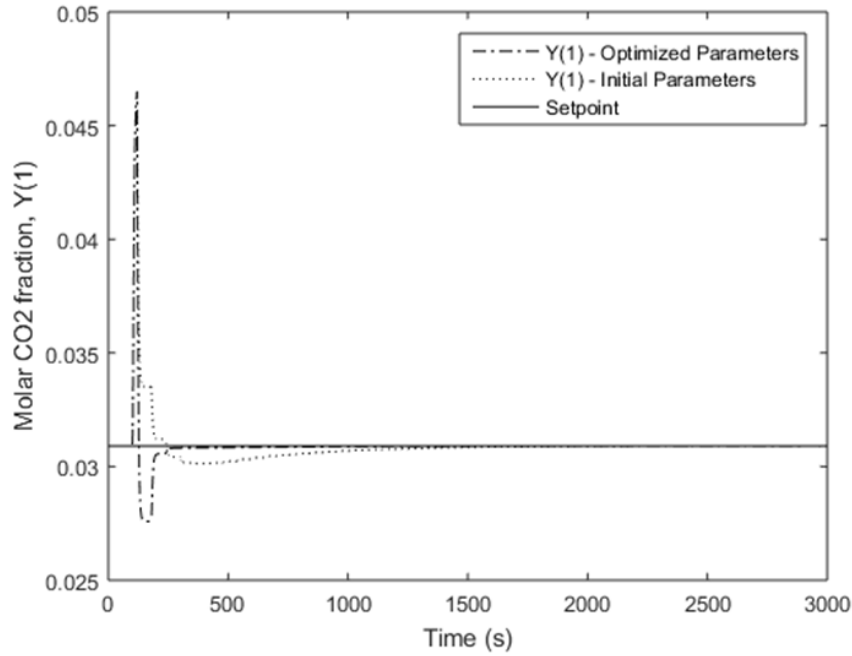


FIGURE 8. Response graph for run 1 with the initial and optimal parameters

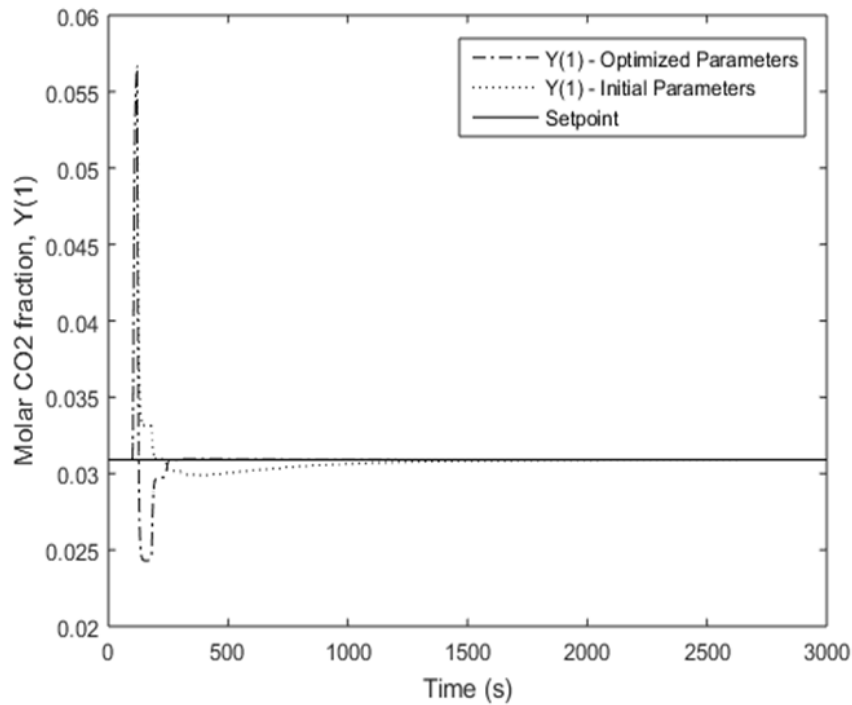


FIGURE 9. Run 2 response chart with initial and optimal parameters

Figure 9 corresponds to the controller response graph for run 2.

In run 2, in which a disturbance 30% higher than that of the CCRD was inserted, the control system also worked effectively, though as reflected by the ITAE value, the error was slightly higher. The ITAE value for optimized parameters was 16% lower than the value for the initial estimate parameters. Using those, the controller took about 750 s more to return to set point (1000 s against 250 s).

The controller response graph for run 3 is shown in Figure 10.

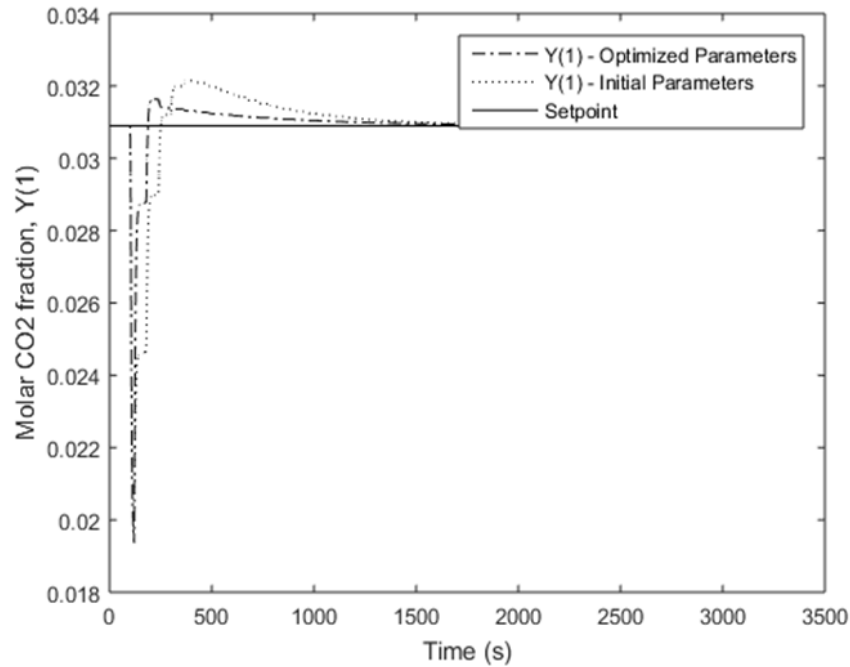


FIGURE 10. Run 3 response graph with initial and optimal parameters

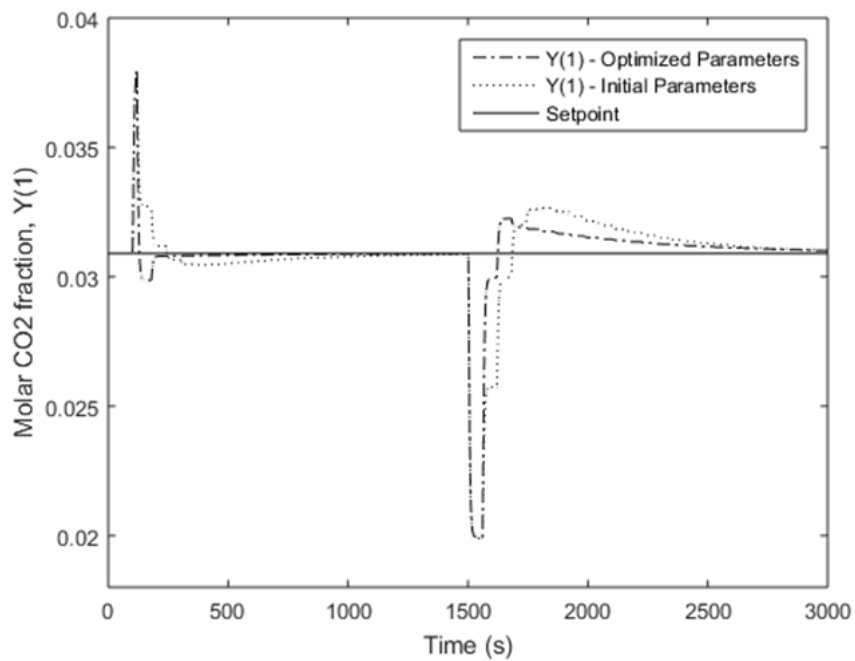


FIGURE 11. Run 4 response graph with initial and optimal parameters

In Test 3, wherein the inserted perturbation had the same magnitude of run 1, though a negative rather than positive one, also showed good results with the optimized parameters. However, due to the disturbance characteristics, the time lapse in which the controlled variable value remains above set point is higher. Again, it is possible to see that the control system showed few oscillations and an error lower than that of the simulation with the initial estimate parameters, which is a reduction of about 58% in ITAE.

The controller response graph for run 4 is shown in Figure 11.

In run 4, it was initially inserted a disturbance similar to that of the CCRD, and after the system was stable, another of equal magnitude, except negative, was inserted. This simulation was particularly interesting because it allowed to verify the control system response to the insertion of successive disturbances, which are very common in real scale. Even in this situation the controller proved its stability, making the controlled variable return to the set point after both perturbations.

Regarding the simulation with the initial parameters, there was a 38% reduction in ITAE value, which can be visualized in the graph (Figure 11). For the first disturbance the controller with the optimal conditions returned to set point in approximately 250 s, as opposed to about 1000 s with the initial conditions. As for the second disturbance, the time to return to set point was 2750 s against around 3000 s.

Therefore, the values found for the controller parameters using the experimental design methodology proved adequate and provided a better performance of the controller than the values with the initial estimate, keeping the system stable even after the introduction of different disturbances, and usually presenting a relatively low accumulated error, as well as few oscillations until it reaches set point.

4. Conclusions. This work aimed to simulate the implementation of a control system in a biogas purification system for carbon dioxide removal, optimizing the tuning of its parameters through a novel methodology for this purpose: the experimental design.

The viability of the use of experimental design methodology to tune PID controller parameters for the studied system was proved. The use of CCDR made it possible to identify which parameters are statistically significant within the study range, obtain optimal regions for the parameters, obtain a quadratic model of the ITAE performance criterion as a function of the significant variable K_c , which was proved valid and predictive to the range through the ANOVA test, as well as through experimental validation, and find optimal values for the controller parameters. The control system with these values had its performance proven solid through simulations with the insertion of disturbances of various magnitudes, in which, as a whole, the controlled variable was stabilized at the set point within short time lapses, while presenting a low accumulated error value, as well as few oscillations.

As evidenced by the graphs shown in this paper, the correct selection for the parameter values is essential in order for a PID control system to present a good performance. Thus, the availability of a methodology that enables good results while requiring fewer tests than the traditional methods (trial and error), and that in addition, presents a statistical basis, appears to be highly advantageous. With its efficiency now proven for PID controller tuning, this methodology could be tested in more complex problems within the systems control field, some of which were mentioned previously, such as finding global optimal values for both servo and regulatory problems, as well as for MIMO plants.

Acknowledgment. The authors would like to thank FUNDAÇÃO ARAUCARIA and CAPES (Coordenação de Aperfeiçoamento de Pessoal de Nível Superior) for its financial support.

REFERENCES

- [1] C. R. Madhuranthakam, A. Elkamel and H. Budman, Optimal tuning of PID controllers FOPR, FOPTD, SOPTD and SOPTD with lead processes, *Chemical Engineering and Processing: Process Intensification*, vol.47, no.2, pp.251-264, 2008.
- [2] M. P. Kumar and M. S. M. Kumar, Tuning of PID controllers for water networks – Different approaches, *Journal AWWA*, vol.101, no.7, 2009.

- [3] G. Chong and Y. Li, PID control system analysis, design, and technology, *Control Systems Technology*, vol.13, no.4, pp.559-576, 2005.
- [4] J. G. Ziegler and N. B. Nichols, Optimum settings for automatic controllers, *Trans. ASME*, vol.64, pp.759-768, 1942.
- [5] H. Cohen and G. A. Coon, Theoretical consideration of retarded control, *Trans. ASME*, vol.75, pp.827-834, 1953.
- [6] A. M. López, J. A. Miller, C. L. Smith and P. W. Murril, Tuning controllers with error-integral criteria, *Instrumentation Technology*, vol.14, pp.57-62, 1967.
- [7] V. M. A. Ruíz, Métodos de sintonización de controladores PID que operan como reguladores, *Ingeniería*, vol.1, no.2, pp.21-36, 2002.
- [8] G. P. Liua and S. Daleyb, Optimal-tuning PID control for industrial systems, *Control Engineering Practice*, vol.9, no.11, pp.1185-1194, 2001.
- [9] K. J. Åström and T. Hägglund, The future of PID control, *Control Engineering Practice*, vol.9, no.11, pp.1163-1175, 2001.
- [10] V. Duarte and J. S. da Costa, Tuning of fractional PID controllers with Ziegler-Nichols-type rules, *Signal Processing*, vol.86, no.10, pp.2771-2784, 2006.
- [11] X. Yang, Y. Li, Y. Kansha and M.-S. Chiu, Enhanced VRFT design of adaptive PID controller, *Chemical Engineering Science*, vol.76, no.9, pp.66-72, 2012.
- [12] O. Arrieta, R. Vilanova, J. D. Rojas and M. Meneses, Improved PID controller tuning rules for performance degradation/robustness increase trade-off, *Electrical Engineering*, vol.98, no.3, pp.233-243, 2016.
- [13] H. S. Sánchez, A. Visioli and R. Vilanova, Optimal Nash tuning rules for robust PID controllers, *Journal of the Franklin Institute*, vol.354, no.10, pp.3945-3970, 2017.
- [14] S. Boyd, M. Hast and K. J. Åström, MIMO PID tuning via iterated LMI restriction, *International Journal of Robust and Nonlinear Control*, vol.26, no.8, pp.1718-1731, 2016.
- [15] D. Kaya and F. Ç. Kiliç, Renewable energies and their subsidies in Turkey and some EU countries – Germany as a special example, *J. Int. Environmental Application & Science*, vol.7, pp.114-127, 2012.
- [16] M. L. O. Maia, *Controle Preditivo de Colunas de Absorção*, UNICAMP, Campinas, 1994.
- [17] E. Eyng and A. M. F. Fileti, Control of absorption columns in the bioethanol process: Influence of measurement uncertainties, *Engineering Applications of Artificial Intelligence*, vol.23, no.2, pp.271-282, 2010.
- [18] Fachagentur Nachwachsende Rohstoffe E.V. (FNR), *Guia prático do Biogás*, 5th Edition, 2010.
- [19] Y. Xiao, H. Yuan, Y. Pang, S. Chen, B. Zhu, D. Zou, J. Ma, L. Yu and X. Li, CO₂ removal from biogas by water washing system, *Chinese Journal of Chemical Engineering*, vol.22, pp.950-953, 2014.
- [20] E. A. Magalhães, S. N. M. Souza, A. D. L. Afonso and R. P. Ricieri, Confecção e avaliação de um sistema de remoção de CO₂ no biogás, *Acta Scientiarum-Technology*, vol.26, no.1, pp.11-19, 2004.
- [21] F. R. Spellman and N. E. Whiting, *Environmental Engineer's Mathematics Handbook*, CRC Press LCC, 2004.
- [22] G. E. P. Box and J. Wetz, *Criteria for Judging Adequacy of Estimation by an Approximate Response Function*, University of Wisconsin Technical Report, no.9, 1973.